Heliyon 10 (2024) e33072

Contents lists available at ScienceDirect

Heliyon

journal homepage: www.cell.com/heliyon

Research article

Transcriptomic and proteomic investigations identify PI3K-akt pathway targets for hyperthyroidism management in rats via polar iridoids from *radix Scrophularia*

Ning Zhang [a], Shumin Liu [b,**], Xu Lu [c], Zihui Li [d], Ling Li [a], Tao Ye [a,*]

[a] *The First Affiliated Hospital of Guizhou University of Traditional Chinese Medicine, Guiyang, Guizhou, China*
[b] *Institute of Traditional Medicine, Heilongjiang University of Chinese Medicine, Harbin, Heilongjiang, China*
[c] *Guizhou University of Traditional Chinese Medicine, Guiyang, Guizhou, China*
[d] *Dalian University, Dalian, China*

ARTICLE INFO

Keywords:
Highly polar iridoids from *radix scrophulariae*
Transcriptomics
Proteomics
Hyperthyroidism
PI3K-Akt signaling pathway

ABSTRACT

High-polarity iridoids from *Radix Scrophulariae* (*R. Scrophulariae*) offer a range of benefits, including anti-inflammatory, antioxidant, antitumour, antibacterial, antiviral, and antiallergic effects. Although previous studies have indicated the potential of *R. Scrophulariae* for hyperthyroidism prevention and treatment, the specific active compounds involved and their mechanisms of action are not fully understood. This study explored the effects of high-polarity iridoid glycosides from *R. Scrophulariae* on hyperthyroidism induced in rats by levothyroxine sodium. The experimental design included a control group, a hyperthyroidism model group, and a group treated with iridoid glycosides. Serum triiodothyronine (T3) and thyroxine (T4) levels were quantified using an enzyme-linked immunosorbent assay (ELISA). Transcriptomic and proteomic analyses were applied to liver samples to identify differentially expressed genes and proteins. These analyses were complemented by trend analysis and Kyoto Encyclopedia of Genes and Genomes (KEGG) enrichment analysis. The effectiveness of key factors was further examined through molecular biology techniques. ELISA results indicated a notable increase in T3 and T4 in the hyperthyroid rats, which was significantly mitigated by treatment with iridoid glycosides. Transcriptomic analysis revealed 6 upregulated and 6 downregulated genes in the model group, showing marked improvement following treatment. Proteomic analysis revealed changes in 30 upregulated and 50 downregulated proteins, with improvements observed upon treatment. The PI3K-Akt signalling pathway was investigated through KEGG enrichment analysis. Molecular biology methods verified the upregulation of Spp1, Thbs1, PI3K, and Akt in the model group, which was reversed in the treatment group. This study revealed that highly polar iridoids from *R. Scrophulariae* can modulate the Spp1 gene and Thbs1 protein via the PI3K-Akt signalling pathway, suggesting a therapeutic benefit for hyperthyroidism and providing a basis for drug development targeting this condition.

* Corresponding author.
** Corresponding author.
E-mail addresses: keji-liu@163.com (S. Liu), yetao008@gzy.edu.cn (T. Ye).

https://doi.org/10.1016/j.heliyon.2024.e33072
Received 6 February 2024; Received in revised form 12 June 2024; Accepted 13 June 2024
Available online 14 June 2024

1. Introduction

Hyperthyroidism is a common thyroid disorder characterized by an overactive thyroid gland, resulting in excessive hormone secretion and an increased metabolic rate. The financial burden and impact on productivity for more than 200 million individuals worldwide affected by hyperthyroidism are significant. Symptoms such as fatigue, anxiety, and palpitations can significantly affect patients' daily lives and work performance [1].

Research has demonstrated that individuals with hyperthyroidism experience a substantial decrease in work capacity and productivity, ranging from 10 % to 30 %, compared to those without hyperthyroidism. Additionally, they may encounter difficulties with concentration and memory, which can have a negative impact on their educational outcomes [2]. Moreover, studies have indicated that hyperthyroidism patients exhibit lower academic performance, reduced learning abilities, and memory deficits. Psychological issues such as anxiety and depression are also prevalent among this population, with approximately 30 %–40 % of people experiencing symptoms that can affect their social and interpersonal relationships [3].

Studies have shown an association between hyperthyroidism and higher rates of miscarriage and premature birth, which impose additional burdens on families and society. Hyperthyroidism has various detrimental effects on individuals and society, including impacts on health, work capacity, learning, mental health, fertility, and family life [4].This highlights the importance of raising awareness, early diagnosis, and effective treatment of hyperthyroidism.

Current treatments for hyperthyroidism in humans include medications, radioactive iodine therapy, and surgery. However, these approaches may have adverse effects and may prove ineffective in certain cases. *Radix Scrophulariae*, also known as *Scrophularia ningpoensis* Hemsl., is a medicinal plant root renowned for its therapeutic qualities, including heat clearing, blood cooling, Yin-nourishing, fire reducing, detoxifying, and nodule dispersing properties. It has been applied in the treatment of various ailments, such as skin eruptions, restlessness, sore throat, and abscesses [5]. *R. Scrophulariae* contains more than 160 compounds, with iridoid glycosides accounting for the principal active constituents. Extensive research has demonstrated the anti-inflammatory, antioxidant, anticancer, antibacterial, antiviral, and antiallergic effects of these glycosides [6]. Previous studies have indicated the potential of *R. Scrophulariae* for the management of hyperthyroidism [7,8], but further investigations are crucial for comprehensively comprehending the specific substances and mechanisms involved.

In recent years, there has been a growing interest in employing in silico techniques to identify potential natural compounds for the prevention and treatment of hyperthyroidism. These techniques rely on computer simulations and modeling to project interactions between bioactive compounds and biological targets, enabling scientists to scrutinize vast compound databases for potential candidates [9–11]. For instance, molecular dynamics simulations have been utilized to reveal the damaging impacts of genetic mutations on protein structure and function, aiding in the prediction of therapeutic targets [12]. Additionally, computational approaches such as SNP analysis have advanced our understanding of the genetic variations associated with diseases, contributing to the development of personalized medicine [13,14]. These advanced techniques facilitate the identification of bioactive compounds with high therapeutic potential and low adverse effects. However, the complex composition of traditional Chinese medicine poses challenges for conducting comprehensive research, impeding the elucidation of drug targets and mechanisms. By utilizing transcriptomics and proteomics to analyse changes in mRNA and protein expression, this study aimed to elucidate the mechanism of *R. Scrophulariae* in treating hyperthyroidism, thus providing a scientific basis for its development.

Therefore, the objective of this study was to explore the mechanism of action of highly polar iridoids from *R. Scrophulariae* in preventing and treating propylthiouracil-induced hyperthyroidism in rats. By integrating transcriptomics and proteomics data, this study will uncover the concealed implications and patterns within the data, elucidating the essence of hyperthyroidism and revealing the mechanism of action of high-polarity iridoid glycosides from *R. Scrophulariae* in preventing and treating hyperthyroidism.

2. Materials and methods

2.1. Plant material and extract preparation

The plant species *R. Scrophulariae*, scientifically known as *Scrophularia ningpoensis* Hemsl., was obtained from Tianjin Shengshi Pharmaceutical Co., Ltd. (Batch No. X220607018). The identification was conducted by Chen Xiumin, the chief pharmacist of the Department of Pharmacy at the First Affiliated Hospital of Guizhou University of Traditional Chinese Medicine, and it adheres to the standards set forth in the 2020 edition of the Pharmacopoeia of the People's Republic of China, page 121. The drugs used in this study were obtained from previous experiments conducted by the research group. The preparation method was as follows: *R. Scrophulariae* was extracted using petroleum ether, and the resulting extract was decocted 10 times or 8 times the amount of water. The decoction liquids were then combined to obtain the water decoction group. The residue of *R. Scrophulariae* extracted with petroleum ether underwent water extraction and alcohol precipitation. The supernatant was passed through D101 macroporous resin, and the water fraction and 10 % ethanol eluate were combined to obtain the highly polar diterpenoid lactone components. These components were subjected to freeze-drying, resulting in the production of a lyophilized powder. In this study, specific highly polar iridoids from *R. Scrophulariae*, including harpagide, harpagoside, and aucubin, were used. According to the 2020 edition of the Chinese Pharmacopoeia, the maximum daily dosage of *R. scapulariae* for adults is 15 g. The yield rate was 50.7 %, which is equivalent to 1.35 g of crude herb per kilogram. The highly polar iridoids from *R. Scrophulariae* constitute 89.25 % of the herb, amounting to 1204.8 mg of crude herb per kilogram [15].

2.2. Animal modelling and administration

Specific pathogen-free (SPF)-grade Sprague–Dawley (SD) rats, consisting of 30 male rats weighing 180–220 g, were provided by Hunan Slake Jingda Experimental Animal Co., Ltd. (Certificate No. SCXK (Xiang) 2019-0004). The animals were housed in the Animal Experimental Center of Heilongjiang University of Traditional Chinese Medicine at a controlled temperature range of 20–25 °C, relative humidity of 40–60 %, and 12-h periods of darkness and light. The rats were provided with ad libitum access to food and water. The use and care of all experimental rats strictly adhered to the relevant provisions of the Animal Protection Association. The Laboratory Animal Ethics Committee of Heilongjiang University of Traditional Chinese Medicine authorized this experiment in accordance with the law on the protection of laboratory animals (Directive 86/609/EEC). After a 7-day adaptation period, the 30 rats were divided into three groups: the control group (K), hyperthyroidism model group (M), and high-polarity iridoid glycoside component (L) administration group, with 10 rats in each group. The control group was fed normally and given oral physiological saline twice in the morning, with an interval of 90 min. The hyperthyroidism model group was given an oral suspension of 120 mg/kg/day of Euthyrox® (levothyroxine sodium tablets, batch no. G01RHA; manufacturer: Merck KGaA) in the morning, followed by oral physiological saline 90 min later, once a day for 15 consecutive days. The high-polarity iridoid group was orally administered highly polar iridoids from *R. Scrophulariae* at a dose of 1205 mg/kg/day, and the remaining procedure was the same as that used for the model group. The signs and symptoms of each group of rats were observed and recorded.

2.3. Sample collection and processing

Twenty-four hours after the final dose, the rats were euthanized under anaesthesia using 1 % pentobarbital sodium (0.15 ml/100 g), and blood was collected from the abdominal aorta. The liver tissues were carefully removed, weighed precisely, and promptly placed in liquid nitrogen. The samples were then frozen and stored at −80 °C for transcriptomic and proteomic analysis.

2.4. ELISA analysis

The blood serum of the rats was centrifuged at 3500 rpm for 10 min at 4 °C to obtain the supernatant. Enzyme-associated immunosorbent assays (ELISAs) were used to measure the levels of T3 (No. 20200720, Nanjing Jiancheng Bioengineering Institute) and T4 (No. 20200720, Nanjing Jiancheng Bioengineering Institute) in rat serum. The experimental procedures strictly followed the corresponding instructions.

2.5. Transcriptomic analysis

For transcriptomic analysis, three liver tissue samples were selected from the control group, hyperthyroidism model group, and high-polarity iridoids from *the R. Scrophularia* administration group. The animal liver tissues frozen at −70 °C were fully ground in liquid nitrogen, and total RNA was extracted using a TRIzol reagent kit (15596026, Invitrogen Life Technologies). The RNA was dissolved in RNase-free water, and RNA integrity was assessed using an RNA 6000 Nano Kit 5067-1511 (5067-1511, Agilent) on an Agilent 2100 Bioanalyzer (Agilent, USA). RNA purity was determined using a Thermo Scientific NanoDrop 2000. The values of the genes aligned to the genome were quantified using HiSeq (http://www-huber.embl.de/users/anders/HiSeq), and differentially expressed genes (DEGs) were analysed using DESeq (http://www-huber.embl.de/users/anders/DESeq). Genes with $|\log_2(\text{fold change})|>1.5$ and significance levels ($P < 0.05$) were selected as DEGs. Annotation information and reads per kilobase million (RPKM) values for each gene were included. The union of the differential expression gene lists from all groups underwent gene and sample biclustering using the R software package pheatmap. Gene Ontology (GO) classification was performed using the targeted GOSlim database. The metabolic pathway information of the genes was obtained from the Kyoto Encyclopedia of Genes and Genomes (KEGG) database.

2.6. Proteomic analysis

Liver tissue samples from each group of rats (3 samples per group as biological replicates) were treated with SDT lysis buffer (4 % SDS, 100 mM Tris-HCl, 1 mM DTT, pH 7.6). After homogenization, the samples were sonicated and subjected to boiling water bath lysis. The supernatant was collected by centrifugation at 14,000×*g* for 45 min at 25 °C. Protein quantification was performed using the BCA method. The samples were then treated with UA (8 M urea, 150 mM Tris-HCl, pH 8.0), IAA (Bio-Rad, 163–2109), and trypsin buffer at 37 °C for 16–18 h. Peptide quantification was measured at OD_{280}. All labelled peptides were mixed and prefractionated using SCX (SCX Buffer A: 10 mM KH2PO4 pH 3.0, 25 % acetonitrile (ACN); SCX Buffer B: 10 mM KH2PO4 pH 3.0, 500 mM KCl, 25 % ACN). Desalting was carried out using a C18 cartridge (66872-U, Sigma) after freeze-drying.

Each sample was separated using the nanoflow HPLC liquid phase system EasynLC. The buffer consisted of Solution A (0.1 % formic acid in water) and Solution B (0.1 % formic acid in an acetonitrile-water solution with 84 % acetonitrile). The chromatographic column was equilibrated with 95 % Solution A. The samples were loaded onto a Thermo Scientific EASY column (2 cm*100 μm 5 μm-C18) and then separated using a Thermo Scientific EASY column (75 μm*100 mm 3 μm-C18) at a flow rate of 300 nl/min. The following liquid phase gradient was used: 0 min–55 min, linear gradient of Solution B from 0 % to 40 %; 55 min–58 min, linear gradient of Solution B from 40 % to 100 %; and 58 min–60 min, Solution B maintained at 100 %. Each sample was analysed using a Q Exactive mass spectrometer (Thermo Finnigan) following separation by capillary high-performance liquid chromatography. The analysis lasted for

60 min, and the detection mode was positive ion mode. The mass range for the parent ion scan was 300–1800 *m/z*, with a primary mass resolution of 70,000 at m/z 200. The AGC target was set to 3e6, and the primary maximum IT was 10 ms. There was only one scan range, and dynamic exclusion was set to 40.0 s. Peptides and peptide fragments were collected using the following method: 10 fragment spectra (MS2 scan) were collected after each full scan. The MS2 activation type was HCD, the isolation window was 2 *m/z*, the secondary mass resolution was 17,500 at m/z 200, and the number of microscans was set to 1. The secondary maximum IT was 60 ms, the normalized collision energy was 30 eV, and the underfill ratio was 0.1 %.

Differentially expressed proteins (DEPs) were selected based on a peptide false discovery rate (FDR) of less than 0.01, a P value of less than 0.05, and a ratio greater than 1.2 or less than 0.833. The selected proteins were then analysed using databases such as Quick GO for gene ontology analysis, KEGG pathways for pathway analysis, and STRING for protein−protein interaction analysis.

2.7. Transcriptomic and proteomic correlation analysis

Transcriptomic and proteomic correlation analyses were conducted to identify commonalities using cross-validation methods, which are scientifically significant. The gene pathway information and protein pathway information affected by the high-polarity iridoid glycosides from *R. Scrophulariae* were integrated into a systematic network.

2.8. Real-time quantitative reverse transcription polymerase chain reaction (qRT−PCR)

qRT−PCR was performed using TRIzol reagent (15596026, Invitrogen Life Technologies) to extract total RNA from rat liver samples, and cDNA was synthesized using a cDNA reverse transcription kit (Qiagen, Valencia, CA, USA) and then used for PCR with specific primers. The amplification conditions were as follows: 95 °C, 2 min (95 °C, 15 s; 60 °C, 1 min) and 40 cycles. Real-time qPCR was performed using the 7300 Real-Time PCR System, as indicated in Table 1. The experiment was repeated three times, with each reaction performed in triplicate. The relative expression levels of mRNA were determined using the $2^{-\triangle\triangle CT}$ method, and statistical significance was considered at $P \leq 0.05$.

2.9. Statistical analysis

The results are presented as ± s. The data were analysed using SPSS 26.0 software. The statistical significance of differences between two groups was analysed using the Bonferroni method or among multiple groups by one-way analysis of variance (ANOVA). A significance level of $P < 0.05$ was considered statistically significant.

3. Results

3.1. Effects of high-polarity iridoid glycosides from R. Scrophulariae on T3 and T4 levels in hyperthyroidism rats

Compared to those in the control group, the serum levels of T3 and T4 in the model group were significantly greater ($P < 0.05$ for T3, $P < 0.01$ for T4). However, treatment with high-polarity iridoid glycosides from *R. Scrophulariae* resulted in a significant decrease in the T3 and T4 levels compared to those in the model group ($P < 0.05$ for T3, $P < 0.01$ for T4) (Fig. 1).

3.2. Transcriptional level DEG trend analysis

In the model group, a total of 86 DEGs were identified, with 36 upregulated and 50 downregulated genes (Fig. 2A–B), compared to those in the control group. After intervention with high-polarity iridoid glycosides from *R. Scrophulariae*, 111 DEGs were identified, including 38 upregulated and 73 downregulated genes, compared to those in the model group (Fig. 2C–D). Twelve DEGs were found to be common among the control group, model group, and *R. Scrophulariae* intervention group. Among these 12 genes whose expression tended to increase, 6 were upregulated in the control group compared to the model group and downregulated in the model group compared to the treatment group, while the remaining 6 genes showed the opposite pattern (fold change >2 or < 0.83, P value < 0.05)

Table 1
Primer sequences.

Gene	Sequence
Spp1	F:5′- CUAGAUGUCGGUGUCCCUUGC -3′ R:5′-UGAAUGUUGCUGCGCAUCAUG -3′
Thbs1	F:5’ -AACGTGGATCAGAGGGACAC -3′ R:5’ -GTCATCGTCATGGTCACAGG- 3′
PI3K	F: 5′-ATTTCCAGTGGGTGAGGCAG-3′ R:5′-CTCATGGTAGCCGGTGACTC-3′
Akt	F:5′ -GTGGCAAGATGTGTATGAG-3′ R:5′ -CTGGCTGAGTAGGAGAAC-3′
β-actin	F:5’ -TCCTGTGGCATCCACGAAACT -3′ R:5′-GAAGCATTTGCGGTGGACGAT -3′

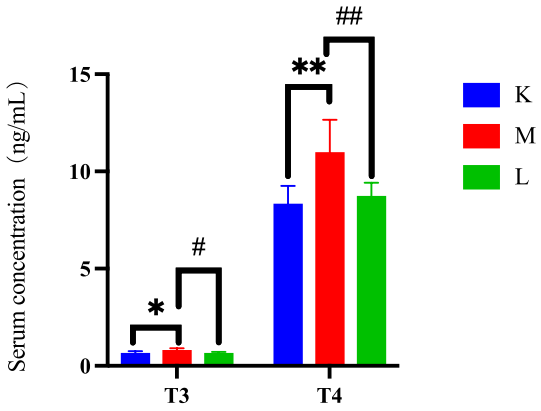

Fig. 1. Effects of high-polarity iridoid glycosides from *R. Scrophulariae* on T3 and T4 levels in hyperthyroidism rats ($\overline{x} \pm s$, n = 10). $^{*}P < 0.05$, $^{**}P < 0.01$ compared to the blank group; $^{\#}P < 0.05$, $^{\#\#}P < 0.01$ compared to the model group.

(Table 2). Biclustering of genes and samples was performed using the R software pheatmap package, combining all the differentially expressed gene lists from the groups. A heatmap of the common DEGs in the three groups is shown in Fig. 3.

3.3. Transcriptional-level GO and KEGG analysis

GO consists of three ontologies that describe the molecular function, cellular component, and biological process of genes. Significant enrichment was observed for enzyme binding, enzyme regulator activity, ion binding, and transcription factor binding in terms of molecular function ($P < 0.05$). Significant enrichment was also observed in the extracellular region, extracellular space, and organelles in terms of cellular components ($P < 0.05$). In terms of biological processes, significant enrichment was observed for anatomical structure development, cell cycle, cell division, cellular protein modification process, growth, immune system process, lipid metabolic process, phosphatase activity, protein binding transcription factor activity, reproduction, response to stress, transferase activity, and alkyl or aryl transfer ($P < 0.05$) (Fig. 4A).

After intervention with high-polarity iridoid glycosides from *R. Scrophulariae*, significant enrichment was detected in lipid metabolism ($P < 0.01$) in terms of metabolism, signal transduction ($P < 0.01$) and signalling molecules and interaction ($P < 0.05$) in terms of environmental information processing; environmental adaptation ($P < 0.01$) in terms of organismal systems; and cancers ($P < 0.01$) and immune diseases ($P < 0.05$) in terms of human diseases (Table 3 and Fig. 4B).

3.4. Protein-level DEP trend analysis

A total of 80 differentially expressed proteins were identified in the three groups, meeting the significance criteria ($P < 0.05$, ratio >1.2 or < 0.833). Among these 80 proteins, 30 were upregulated in the control group compared to the model group and downregulated in the model group compared to the treatment group. Conversely, the remaining 50 proteins showed the opposite pattern (Table 4).

3.5. Protein level GO and KEGG analysis

3.5.1. Protein level GO and KEGG analysis

The 80 differentially expressed proteins identified among the three groups were associated with 171 biological processes ($P < 0.05$), 58 cellular components ($P < 0.05$), 80 molecular functions ($P < 0.05$), and 9 KEGG pathways ($P < 0.05$) (Fig. 5A–D).

3.6. Protein-protein interaction (PPI) network at the protein level

The PPI network of significantly differentially expressed proteins was constructed using the STRING database and Cytoscape 3.8.2. The key proteins identified included p21-activated kinase 1 (Pak1), alcohol dehydrogenase 6 (Adh6), septin 6 (Sept6), DNA-directed RNA polymerase II subunit RPB2 (Polr2*b*), myosin-Vb (Myo5*b*), 3alpha(17beta)-hydroxysteroid dehydrogenase (NAD+) (Hsd17b2), beta-globin chain (Fragment) (Hbg1), hemoglobin subunit alpha 2 (Hba2), Copine 3 (Cpne3), aldehyde dehydrogenase 1 family member A1 (Aldh1a1), autophagy-related 4A, cysteine peptidase (Agt4a), and medium-chain acyl-CoA synthetase 5 (Acsm5) (Fig. 5E).

3.7. Integration analysis of transcriptomics and proteomics

Comparison of the KEGG results from transcriptomic and proteomic trend analysis revealed that key signalling pathways were associated with ovarian steroidogenesis, steroid hormone biosynthesis, focal adhesion, extracellular matrix (ECM)-receptor

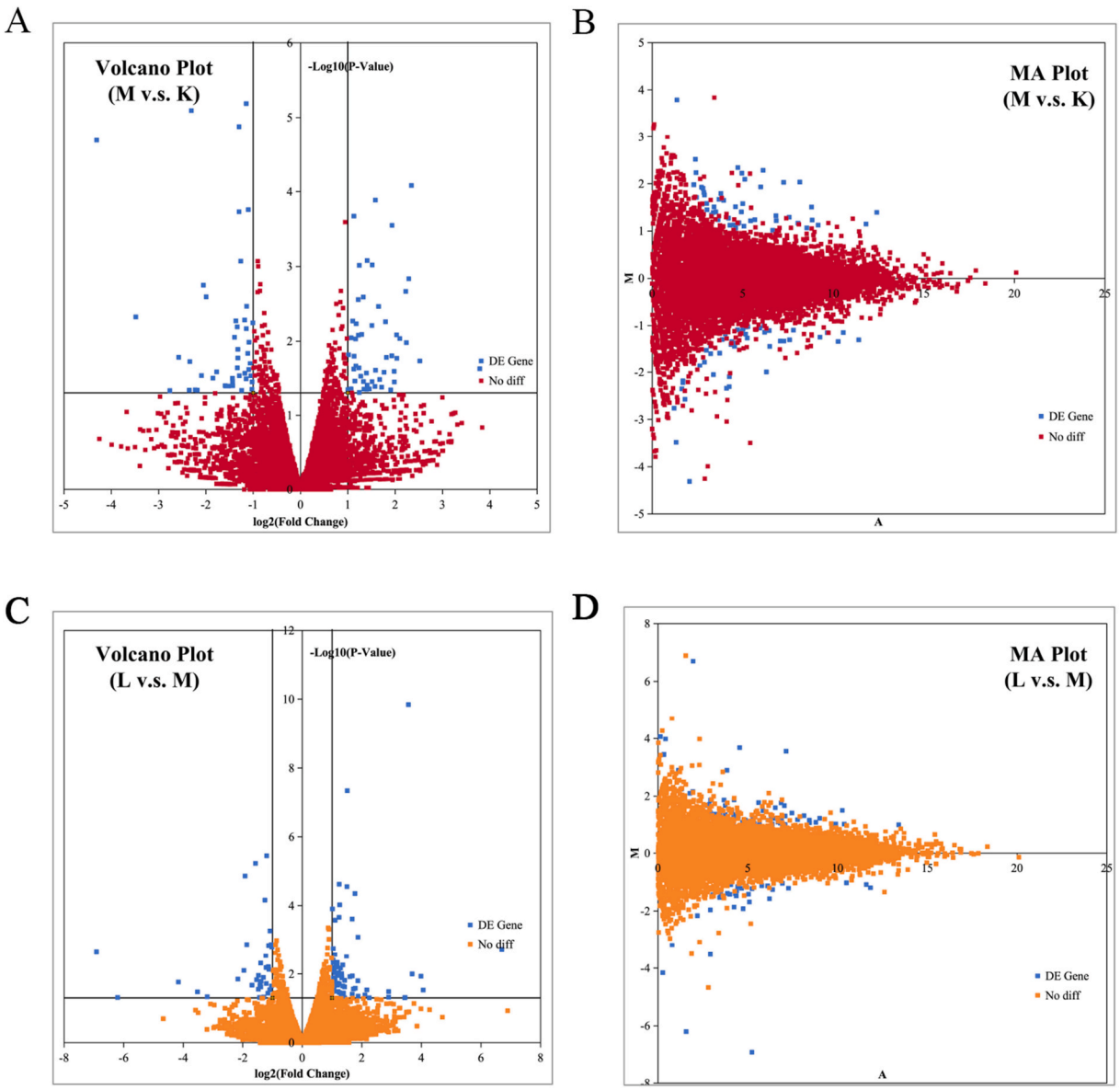

Fig. 2. Volcano plot and MA plot. (A) Volcano plot of levothyroxine sodium tablet (LST)-induced hyperthyroidism rats. The x-axis represents the log-fold change in expression, and the y-axis represents the negative log of the significance of differential expression. The vertical line represents a 2-fold difference threshold, and the horizontal line represents a $P < 0.05$ threshold. Genes that met the differential expression criteria are represented by blue dots, while genes that did not meet the criteria are represented by orange dots. (B) MA plot of the rats with LST-induced hyperthyroidism. The MA plot reflects the trend of expression differences between samples regardless of expression level. (C) Volcano plot of the effects of highly polar iridoids from *R. Scrophulariae* on hyperthyroidism model rats. (D) MA plot of the effects of highly polar iridoids from *R. Scrophulariae* on hyperthyroidism model rats.

interaction, and the PI3K-Akt signalling pathway. In the PI3K-Akt signalling pathway, secreted phosphoprotein 1 (Spp1) was found to be enriched in differentially expressed genes at the transcriptomic level, while protein thrombospondin 1 (Thbs1) was found to be differentially expressed at the proteomic level. Both genes and proteins were significantly downregulated after treatment, consistent with the upregulation caused by modelling. This integrated analysis of genes and proteins in a common pathway provides a more focused direction for further investigation of the mechanism of hyperthyroidism and the intervention effect and mechanism of high-polarity iridoid glycosides from *R. Scrophulariae*.

Table 2
Differentially expressed genes (DEGs) after intervention with high-polarity iridoid glycosides from *Radix Scrophulariae*.

No.	ID	2-Fold Change	gene	Chromosome	Regulation(M vs K)	pval(M vs K)	regulation(L vs M)	pval(L vs M)	Annotation
1	ENSRNOG00000017878	0.45	Aldh1a7	1	Down	0.0035	Up	0.0363	aldehyde dehydrogenase family 1, subfamily A7
2	ENSRNOG00000018059	0.37	Ihh	9	Down	0.0018	Up	0.0189	Indian hedgehog
3	ENSRNOG00000018287	0.44	RGD1307603	1	Down	0.0296	Up	0.0000	similar to hypothetical protein MGC37914
4	ENSRNOG00000050224	0.27	Stambpl1	1	Down	0.0286	Up	0.00 14	STAM binding protein-like 1
5	ENSRNOG00000046487	0.00	Pou5f1	20	Down	0.0369	Up	0.02 21	POU class 5 homeobox 1
6	ENSRNOG00000061779	0.00	Man2b2	14	Down	0.0492	Up	0.0427	mannosidase, alpha, class 2B, member 2
7	ENSRNOG00000009570	2.26	Pdxp	7	Up	0.0170	Down	0.00 46	pyridoxal (pyridoxine, vitamin B6) phosphatase
8	ENSRNOG00000019441	15.83	Hsd3b1	2	Up	0.0396	Down	0.0117	hydroxy-delta-5-steroid dehydrogenase, 3 beta- andsteroid delta-isomerase 1
9	ENSRNOG00000032618	3.03	Mst1r	8	Up	0.0040	Down	0.0121	macrophage stimulating 1 receptor
10	ENSRNOG00000043451	3.67	Spp1	14	Up	0.0388	Down	0.0444	secreted phosphoprotein 1
11	ENSRNOG00000047520	2.39	Rn60_5_0815.11	5	Up	0.0040	Down	0.00 01	Protein LOC100912565
12	ENSRNOG00000059770	103.85	RT1-A3	20	Up	0.0008	Down	0.0019	Uncharacterized protein

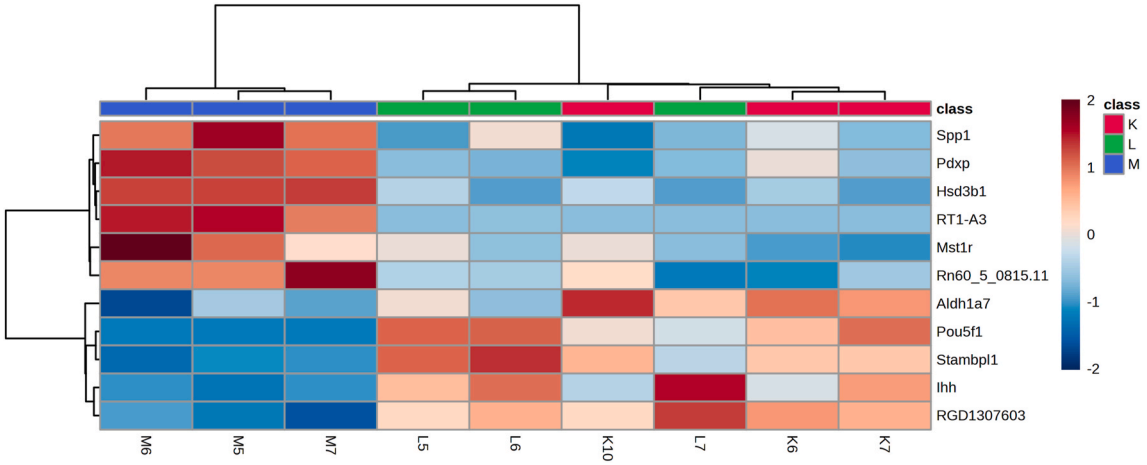

Fig. 3. Heatmap of commonly differentially expressed genes (DEGs) in the control, model, and treatment groups. A heatmap was generated by clustering the RPKM values of DEGs using the median expression value as the median and the Pearson distance method (absolute value) as the clustering method. The red color in the heatmap represents highly expressed genes, while the blue color represents genes with low expression. K represents the control group, M represents the model group, and L represents the group treated with high-polarity iridoid glycosides from *R. Scrophulariae*.

3.8. Verification of the improvement of hyperthyroidism by regulating the PI3K-akt signalling pathway through highly polar iridoids from R. Scrophulariae

The qRT−PCR results demonstrated significant increases in the levels of Spp1, Thbs1, PI3K, and Akt in the model group compared to those in the control group ($P < 0.01$). Conversely, the treatment group exhibited a significant decrease in the levels of these factors compared to those in the model group ($P < 0.01$). These findings affirm the ability of highly polar iridoids from *R. Scrophulariae* to regulate hyperthyroidism by modulating key factors in the pathway. Moreover, these findings suggest that these iridoids may alleviate hyperthyroidism in rats by inhibiting the PI3K/Akt pathway (Fig. 6).

4. Discussion

Transcriptomics and proteomics are valuable tools for studying changes in gene expression levels and validating these findings, respectively, under various conditions, including hyperthyroidism [16,17]. By utilizing the combined application of transcriptomics and proteomics, this study comprehensively analysed gene expression levels, revealed regulatory mechanisms, identified biomarkers, and guided treatment strategies in the context of the preventive and therapeutic potential of R. Scrophulariae for hyperthyroidism. Consequently, this study offers novel insights and methods for advancing research and treatment approaches for hyperthyroidism.

There are several methods available for inducing hyperthyroidism in rats, such as surgical thyroidectomy, the administration of thyroid-stimulating hormone (TSH), and the use of thyroid hormones such as levothyroxine sodium. Levothyroxine sodium, which is a synthetic form of the thyroid hormone T4, is commonly employed for inducing hyperthyroidism in rats due to its potency and ability to rapidly elevate thyroid hormone levels in the body. Typically, levothyroxine sodium is administered orally or intraperitoneally to rats to mimic the effects of hyperthyroidism. This choice is justified by the advantages it offers in terms of precise control over the dosage and timing of thyroid hormone administration, thereby facilitating the induction and maintenance of hyperthyroidism in experimental animals. Additionally, levothyroxine sodium is a stable and well-tolerated form of thyroid hormone that is easily absorbed by the body, making it a reliable option for inducing hyperthyroidism in rats for research purposes. In the early stages of the project, the research group utilized Euthyrox (sodium levothyroxine tablets) to establish a hyperthyroidism model in normal rats. The model was assessed based on physical signs, basal metabolic rate, and relevant indicators in the body, which provided evidence for the scientific validity of this hyperthyroidism model [18].

According to the 2020 edition of the Pharmacopoeia of the People's Republic of China, the recommended maximum daily dose of *R. Scrophulariae* for adult clinical use is 15 g, with an extract yield of 50.7 %. For the experimental rats, the raw herb dosage was 1.35 g/kg. Previous studies conducted by our research group have indicated that *R. Scrophulariae* extract has the ability to target and modulate biomarkers in the blood [19], urine [20,21], and liver [22–24], achieving balance and effectively preventing and treating hyperthyroidism. A significant percentage of *R.* scapulariae is composed of the major polar diterpene glycosides, which account for 89.25 % and are equivalent to 1205 mg of raw herbs/kg/day. Based on these findings, this research group aimed to investigate whether major polar diterpene glycosides are responsible for the pharmacological efficacy of *R. Scrophulariae* in preventing and treating hyperthyroidism.

The decision to use serum levels of T3 and T4 as biomarkers for hyperthyroidism is grounded in the fact that these hormones are primarily produced by the thyroid gland and are essential for regulating metabolism [25]. In cases of hyperthyroidism, excessive

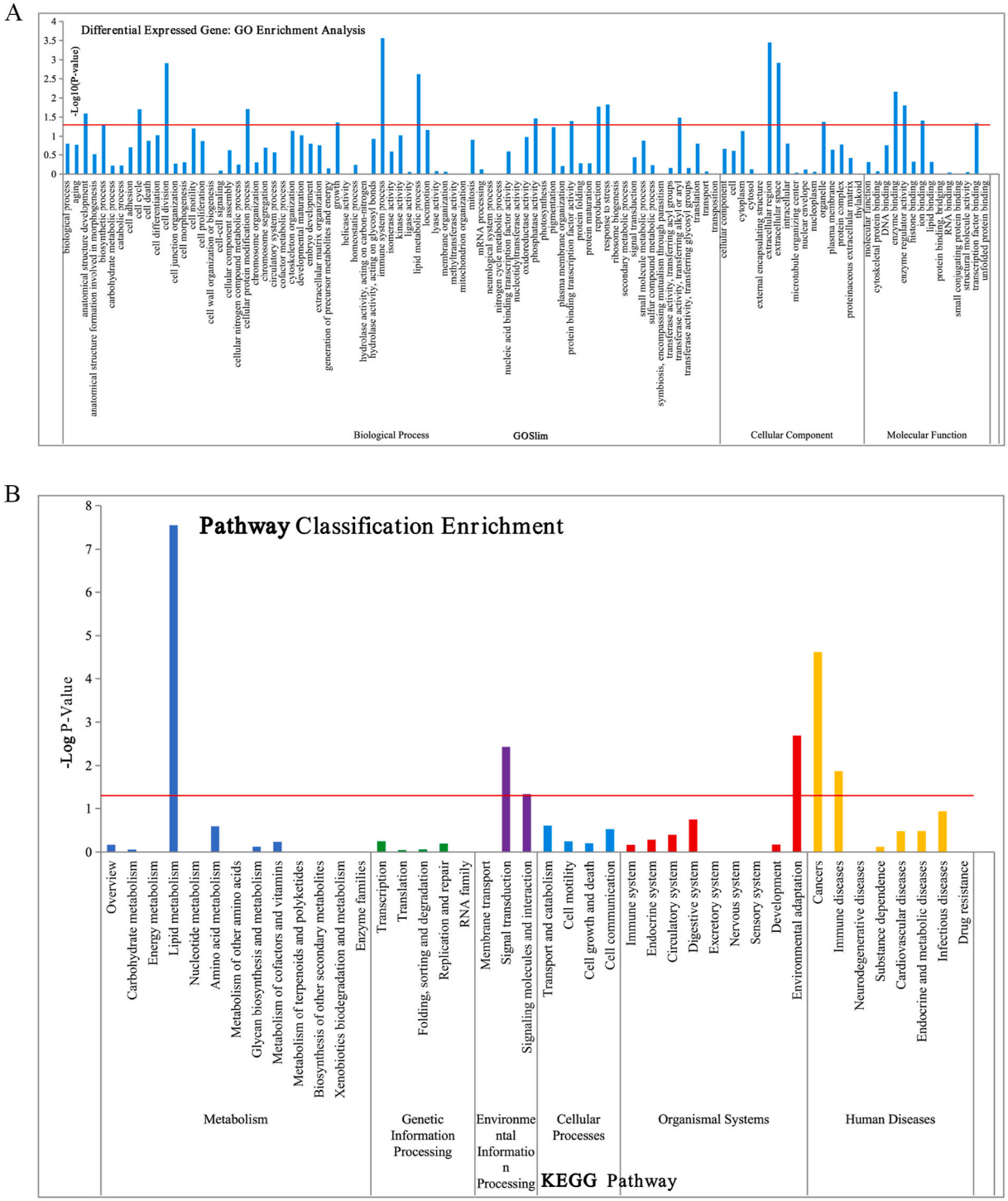

Fig. 4. GO enrichment analysis and pathway classification enrichment. (A) Bar chart showing the enrichment analysis of differentially expressed genes (DEGs) in hyperthyroidism-induced rats treated with highly polar iridoids from *R. Scrophulariae*. The x-axis represents gene GO functional categories, and the y-axis represents the significance of enrichment calculated using the hypergeometric distribution (*P* value). The red line in the graph represents a *P* value = 0.05, indicating the GO functional categories that may be enriched in DEGs compared to the entire gene expression background. (B) KEGG pathway enrichment analysis of DEGs in hyperthyroidism-induced rats treated with highly polar iridoids from *R. Scrophulariae*. The x-axis represents KEGG pathways, and the y-axis represents the significance of enrichment calculated using the hypergeometric distribution (*P* value). The red line in the graph represents a *P* value = 0.05, indicating the KEGG pathways that may be enriched in DEGs compared to the entire gene expression background.

Table 3
Transcriptome-level KEGG enrichment analysis.

NO.	pathway	pathway ID	ID	gene
1	Steroid hormone biosynthesis	ko:K00070	ENSRNOG00000019441	Hsd3b1
2	Vitamin B6 metabolism	ko:K07758	ENSRNOG00000009570	Pdxp
3	Hedgehog signaling pathway	ko:K11989	ENSRNOG00000018059	Ihh
4	PI3K-Akt signaling pathway	ko:K06250	ENSRNOG00000043451	Spp1
5	ECM-receptor interaction	ko:K06250	ENSRNOG00000043451	Spp1
6	Focal adhesion	ko:K06250	ENSRNOG00000043451	Spp1
7	Toll-like receptor signaling pathway	ko:K06250	ENSRNOG00000043451	Spp1
8	Ovarian Steroidogenesis	ko:K00070	ENSRNOG00000019441	Hsd3b1

production of these hormones by the thyroid gland results in symptoms such as weight loss, increased heart rate, and nervousness.

Although iridoid glycosides have promising therapeutic potential, it is crucial to acknowledge the potential off-target effects of these compounds. Individuals considering the use of iridoid glycosides for their health benefits should consult with a healthcare provider. This consultation is essential for discussing the potential risks and benefits, especially if patients have underlying health conditions or are using other medications.

Iridoid glycosides are a class of natural compounds that can be found in various plants, such as those from the *Gentianaceae* and *Apocynaceae* families. Extensive research has been conducted on these compounds to determine their potential therapeutic effects, which include anti-inflammatory, antioxidant, and neuroprotective effects. However, similar to any bioactive compound, iridoid glycosides may also cause off-target effects that could be detrimental.

One possible off-target effect of iridoid glycosides is their interaction with other medications. These compounds have the potential to interfere with the metabolism of certain drugs, leading to altered drug levels within the body. Consequently, this may cause adverse effects or reduce the efficacy of the medications [26]. Therefore, individuals taking iridoid glycosides should inform their healthcare providers about all medications being used to avoid potential drug interactions.

Another plausible off-target effect of iridoid glycosides relates to their impact on the gastrointestinal system. Some individuals may experience gastrointestinal discomfort, such as nausea, vomiting, or diarrhea, when consuming these compounds [27]. This could result from the irritant effects of iridoid glycosides on the digestive tract or their influence on gut motility.

Furthermore, it is important to note the potential effects of iridoid glycosides on the cardiovascular system [28]. Research suggests that these compounds may have a hypotensive effect, resulting in lowered blood pressure. Although this approach may be beneficial for individuals with hypertension, it could be potentially harmful for those with preexisting low blood pressure or those taking medication to lower blood pressure [29].

The differentially expressed genes and proteins identified in hyperthyroidism, such as Spp1, Thbs1, PI3K, and Akt, have significant physiological relevance in the pathophysiology of the disease. Targeting these molecules may provide innovative therapeutic strategies for the management of hyperthyroidism and its associated complications, including bone loss, cardiovascular diseases, and metabolic disorders.

Hyperthyroidism is a condition characterized by an overactive thyroid gland, resulting in excessive production of thyroid hormones. This hormonal imbalance can have diverse effects on various physiological processes within the body. The differentially expressed genes and proteins identified, including Spp1, Thbs1, PI3K, and Akt, play crucial roles in the pathophysiology of hyperthyroidism and are potential therapeutic targets.

Osteopontin (Spp1) is a secreted glycoprotein involved in various physiological processes, such as bone metabolism, the immune response, and inflammation. In the context of hyperthyroidism, Spp1 has been shown to be upregulated and may contribute to the development of osteoporosis, which is a common complication of hyperthyroidism [30]. Targeting Spp1 could aid in preventing bone loss and improving bone health in individuals with hyperthyroidism.

Thbs1 is a matricellular protein that plays a role in cell adhesion, migration, and angiogenesis. In hyperthyroidism, the expression of Thbs1 is dysregulated and may contribute to the development of cardiovascular complications, such as hypertension and cardiac hypertrophy [31]. Targeting Thbs1 could help in preventing cardiovascular complications associated with hyperthyroidism.

The PI3K/Akt signalling pathway is a critical regulator of cell growth, survival, and metabolism. Dysregulation of this pathway has been implicated in various diseases, including cancer and metabolic disorders. In hyperthyroidism, the PI3K/Akt pathway is often activated, leading to increased cell proliferation and metabolic rate [32].Targeting phosphoinositide 3-kinase (PI3K) or Akt (protein kinase B) may help regulate cell growth and metabolism in hyperthyroidism patients, potentially reducing the risk of thyroid cancer and metabolic complications.

The interactions between Spp1, Thbs1, PI3K, and Akt are believed to play a critical role in regulating thyroid function. These interactions can influence thyroid hormone synthesis and secretion, as well as thyroid cell proliferation, differentiation, and survival. Disruption or dysregulation of these key factors can lead to thyroid dysfunction and contribute to thyroid disorders. Spp1, Thbs1, PI3K, and Akt are key factors involved in various cellular processes that can impact the regulation of thyroid function.

SPP1, which encodes osteopontin/secreted phosphoprotein 1, is involved in cell adhesion, migration, signal transduction, inflammation, immune regulation, and bone metabolism [33].Studies have suggested that osteopontin may play a role in the development of hyperthyroidism [34]. Elevated levels of osteopontin have been detected in the serum of hyperthyroid patients, and its expression is positively correlated with thyroid hormone levels. Osteopontin is also involved in thyroid cell proliferation and differentiation, which may contribute to the pathological process of hyperthyroidism [35]. However, further research is needed to fully

Table 4
Significantly different proteins shared among the control group, model group, and highly polar iridoids from *Radix Scrophulariae* group.

No.	Accession	GN	Description	Average RatioM/K	Trends M/K	T Test K Vs M	Average Ratio L/M	Trends L/M	T Test L Vs M
1	Q63066	Hbg1	Beta-globin chain (Fragment)	5.6838	↑	0.0127	0.1459	↓	0.0100
2	G3V8Y5	Polr2b	DNA-directed RNA polymerase	4.0023	↑	0.0008	0.2633	↓	0.0012
3	A0A0G2JSK1	Serpina3c	Protein Serpina3c	2.6222	↑	0.0010	0.6644	↓	0.0161
4	A0A0G2KBC7	Pfkm	ATP-dependent 6-phosphofructokinase	1.9737	↑	0.0497	0.6216	↓	0.0335
5	Q6P7Q6	Lgals9	Galectin	1.5763	↑	0.0463	0.5339	↓	0.0238
6	F1LMF4	Fat3	Protocadherin Fat 3	1.5600	↑	0.0006	0.6169	↓	0.0010
7	P12336	Slc2a2	Solute carrier family 2, facilitated glucose transporter member 2	1.4963	↑	0.0001	0.5445	↓	0.0000
8	A0A0G2K7H6	Serpinb8	Protein Serpinb8	1.4770	↑	0.0000	0.7561	↓	0.0000
9	M0R979	Thbs1	Protein Thbs1	1.4022	↑	0.0113	0.6933	↓	0.0109
10	D4ADS4	Mgst3	Protein Mgst3	1.3882	↑	0.0000	0.7205	↓	0.0000
11	Q99P74	Rab27b	Ras-related protein Rab-27B	1.3769	↑	0.0002	0.5217	↓	0.0002
12	A0A0G2JSV6	Hba2	Protein Hba2	1.3613	↑	0.0006	0.8288	↓	0.0021
13	D4ADQ1	Rrm2b	Protein Rrm2b	1.3592	↑	0.0000	0.7110	↓	0.0000
14	D4A4A8	Invs	Protein Invs	1.3539	↑	0.0000	0.5361	↓	0.0000
15	Q5I0E3		Uncharacterized protein C7orf50 homolog	1.3473	↑	0.0000	0.7918	↓	0.0000
16	Q5M827	Pir	Pirin	1.3325	↑	0.0094	0.6768	↓	0.0438
17	P36860	Ralb	Ras-related protein Ral-B	1.3321	↑	0.0000	0.5972	↓	0.0000
18	P50170	Rdh2	Retinol dehydrogenase 2	1.2944	↑	0.0002	0.6120	↓	0.0000
19	G3V801	Prss12	Neurotrypsin	1.2938	↑	0.0236	0.6913	↓	0.0068
20	A0A0G2K315		Uncharacterized protein	1.2853	↑	0.0034	0.7341	↓	0.0005
21	Q5I0L0	Amy1a	Alpha-amylase	1.2763	↑	0.0013	0.6048	↓	0.0001
22	Q9R2C1	Serp1	Stress-associated endoplasmic reticulum protein 1	1.2638	↑	0.0175	0.8011	↓	0.0016
23	D3ZXX7	Brd7	Bromodomain containing 7 (Predicted)	1.2629	↑	0.0015	0.7472	↓	0.0006
24	A0A0G2JU41	Dyrk4	Protein Dyrk4	1.2607	↑	0.0002	0.7345	↓	0.0001
25	Q562C4	Mettl7b	Methyltransferase-like protein 7B	1.2580	↑	0.0001	0.7699	↓	0.0001
26	P70569	Myo5b	Unconventional myosin-Vb	1.2477	↑	0.0215	0.5930	↓	0.0102
27	D3ZFK8	Farp2	FERM, RhoGEF and pleckstrin domain protein 2 (Predicted)	1.2459	↑	0.0044	0.7562	↓	0.0026
28	B5DFG5	6-Sep	Protein Sept6	1.2418	↑	0.0196	0.8133	↓	0.0227
29	Q925D4	Tmem176b	Transmembrane protein 176B	1.2279	↑	0.0001	0.7582	↓	0.0114
30	Q5HZA7	Bin1	Bin1 protein	1.2018	↑	0.0343	0.7749	↓	0.0284
31	F1LM09	Usp7	Ubiquitin carboxyl-terminal hydrolase	0.8276	↓	0.0111	1.3097	↑	0.0120
32	Q5XIM5	Cdv3	Protein CDV3 homolog	0.8237	↓	0.0018	1.3392	↑	0.0001
33	D3Z8C2	RGD1560028	Protein RGD1560028	0.8171	↓	0.0000	1.4942	↑	0.0000
34	D3Z881	Tbc1d4	Protein Tbc1d4	0.8168	↓	0.0001	1.3351	↑	0.0000
35	A0A0G2K3G9	Ppp1r10	Serine/threonine-protein phosphatase 1 regulatory subunit 10	0.8163	↓	0.0000	1.3392	↑	0.0000
36	D4AAT4	Snrpf	Protein Snrpf	0.8146	↓	0.0206	1.4473	↑	0.0011
37	F1M0A6	LOC100909750	Non-specific protein-tyrosine kinase	0.8119	↓	0.0281	1.6425	↑	0.0045
38	Q91XJ1	Becn1	Beclin-1	0.8113	↓	0.0000	1.2024	↑	0.0000
39	A0A0G2JVS3	Zbtb44	Zinc finger and BTB domain-containing protein 44	0.8076	↓	0.0485	1.4413	↑	0.0161
40	A0A0G2K7W8	Hint3	Histidine triad nucleotide-binding protein 3	0.8046	↓	0.0105	1.2217	↑	0.0034
41	Q6AYT9	Acsm5	Acyl-coenzyme A synthetase ACSM5, mitochondrial	0.8032	↓	0.0014	1.2430	↑	0.0016
42	F6QBA3	Plin2	Perilipin	0.7963	↓	0.0084	1.5992	↑	0.0004
43	B0BN90	Dimt1	DIM1 dimethyladenosine transferase 1-like (*S. cerevisiae*)	0.7936	↓	0.0237	1.5426	↑	0.0174
44	D4AE35	Sult2a1	Sulfotransferase	0.7931	↓	0.0045	3.6274	↑	0.0000
45	D3ZLA3	Cpne3	Copine 3 protein	0.7911	↓	0.0010	1.3940	↑	0.0003
46	F7FLV0	LOC501618	Protein LOC501618	0.7893	↓	0.0000	1.2194	↑	0.0000
47	P49890	Ste2	Estrogen sulfotransferase Ste2	0.7861	↓	0.0130	1.3401	↑	0.0009
48	F1LRQ7	Slc21a4	Solute carrier organic anion transporter family member	0.7818	↓	0.0064	1.4618	↑	0.0003
49	P35465	Pak1	Serine/threonine-protein kinase PAK 1	0.7727	↓	0.0000	1.3674	↑	0.0000
50	D4A2D7	Ipo4	Importin 4 (Predicted), isoform CRA_b	0.7716	↓	0.0054	1.2178	↑	0.0162

(*continued on next page*)

Table 4 (*continued*)

No.	Accession	GN	Description	Average RatioM/K	Trends M/K	T Test K Vs M	Average Ratio L/M	Trends L/M	T Test L Vs M
51	A0A0G2KAJ7	Col12a1	Collagen alpha-1(XII) chain	0.7646	↓	0.0093	1.9153	↑	0.0002
52	A0A0G2JXL0	Pitpnm2	Protein Pitpnm2	0.7624	↓	0.0000	2.4385	↑	0.0000
53	P06302	Ptma	Prothymosin alpha	0.7609	↓	0.0076	1.5783	↑	0.0040
54	F1M7P8	Spryd3	Protein Spryd3	0.7580	↓	0.0008	1.6907	↑	0.0000
55	Q5XI95	Adh6	Alcohol dehydrogenase 6	0.7512	↓	0.0059	1.4916	↑	0.0036
56	G3V7V6	Retsat	All-trans-13,14-dihydroretinol saturase, isoform CRA_b	0.7435	↓	0.0002	1.3153	↑	0.0001
57	A0A0G2K7X3	Nucks1	Nuclear ubiquitous casein and cyclin-dependent kinase substrate 1	0.7411	↓	0.0011	1.2818	↑	0.0002
58	P0C6B8	Svep1	Sushi, von Willebrand factor type A, EGF and pentraxin domain-containing protein 1	0.7395	↓	0.0029	1.6481	↑	0.0022
59	D4A900	Filip1l	Protein Filip1l	0.7247	↓	0.0000	1.9677	↑	0.0000
60	A0A0G2JUG7	Iqsec1	Protein Iqsec1	0.7235	↓	0.0000	1.6103	↑	0.0000
61	E9PSL8	Kif6	Kinesin-like protein	0.7165	↓	0.0126	1.5028	↑	0.0036
62	M0RBN6	Nrxn1	Neurexin-1-beta (Fragment)	0.7001	↓	0.0000	1.5597	↑	0.0000
63	J7NUQ1	Irgm	Interferon-gamma-inducible GTPase Ifggd3 protein	0.6979	↓	0.0432	1.2953	↑	0.0012
64	D4A7W1	Abhd2	Abhydrolase domain containing 2 (Predicted)	0.6910	↓	0.0000	1.7087	↑	0.0000
65	D4A2D3	Mycbp2	Protein Mycbp2	0.6866	↓	0.0000	2.3203	↑	0.0000
66	M0R9G9	Atg4a	Protein Atg4a	0.6846	↓	0.0000	1.3693	↑	0.0000
67	Q6MFZ1	RT1-M1-5	RT1 class I, M1, gene 5 (Fragment)	0.6801	↓	0.0004	1.4803	↑	0.0053
68	D3ZDP4	LOC102548013	Protein LOC102548013	0.6762	↓	0.0182	1.7879	↑	0.0051
69	A4L9P7	Pds5a	Sister chromatid cohesion protein PDS5 homolog A	0.6561	↓	0.0036	2.3003	↑	0.0001
70	Q6AYI9	Lrrc23	Leucine rich repeat containing 23	0.6540	↓	0.0008	2.3302	↑	0.0055
71	P13601	Aldh1a7	Aldehyde dehydrogenase, cytosolic 1	0.6066	↓	0.0002	1.5303	↑	0.0004
72	M0R5R3	LOC100910849	Protein LOC100910849	0.5990	↓	0.0000	1.4756	↑	0.0000
73	M0RAS5		Uncharacterized protein	0.5899	↓	0.0029	1.7046	↑	0.0001
74	D3ZJ56	Gbp3	Protein Gbp3	0.5890	↓	0.0078	2.7030	↑	0.0019
75	D4A0U3	Zfp638	Protein Zfp638	0.5866	↓	0.0039	2.0355	↑	0.0018
76	Q4V9H5	Phf20l1	PHD finger protein 20-like protein 1	0.5684	↓	0.0010	2.6287	↑	0.0002
77	Q5I0N4	Hsd17b2	Estradiol 17-beta-dehydrogenase 2	0.5556	↓	0.0000	1.5696	↑	0.0001
78	P58428	Abcg8	ATP-binding cassette sub-family G member 8	0.4951	↓	0.0049	3.3984	↑	0.0012
79	Q6MGD2	Zbtb9	Protein Zbtb9	0.4437	↓	0.0020	3.6411	↑	0.0024
80	M0RDF1	Kdm3b	Protein Kdm3b	0.2927	↓	0.0000	3.9077	↑	0.0000

understand the underlying mechanisms and modes of action involved.

THBS1, also known as thrombospondin 1, is a multifunctional extracellular matrix protein with various biological functions. It is involved in extracellular matrix assembly and regulation, cell migration and proliferation, angiogenesis, and inflammation, among other biological processes [36]. Studies have shown increased expression of THBS1 in the thyroid tissue of hyperthyroid patients [37]. Furthermore, THBS1 in thyroid cells is associated with the synthesis and secretion of thyroid hormones. The upregulation of THBS1 in hyperthyroidism may contribute to the excessive proliferation of thyroid cells and the enhanced synthesis and secretion of thyroid hormones. THBS1 can increase thyroid peroxidase (TPO) expression, thereby facilitating thyroid hormone synthesis and secretion. Moreover, THBS1 can modulate immune responses and contribute to inflammation regulation. Hyperthyroidism frequently coincides with immune system overactivity and heightened inflammation. Elevated THBS1 levels might be associated with these immune irregularities [38].

PI3K, or phosphoinositide 3-kinase, is a key signalling molecule involved in regulating cellular processes such as cell growth, survival, and metabolism. It activates the Akt signalling pathway, which plays a critical role in cell proliferation, survival, and metabolism. In the context of thyroid function, the PI3K/Akt signalling pathway may regulate thyroid hormone synthesis and secretion, as well as thyroid cell proliferation and survival. In patients with hyperthyroidism, the activity of the PI3K signalling pathway is often significantly increased, leading to abnormal proliferation of thyroid cells and increased secretion of thyroid hormones [32]. This could be due to the regulatory effects of thyroid hormones on the PI3K signalling pathway, as well as the regulatory effects of the pathway on the synthesis and release of thyroid hormones.

Akt is a serine/threonine protein kinase that acts as a downstream effector of PI3K signalling. It plays a key role in regulating cellular processes, including cell growth, survival, and metabolism. Akt signalling has been implicated in the regulation of thyroid hormone synthesis, secretion, cell proliferation, and survival. Hyperactivation of the Akt signalling pathway promotes cell proliferation, inhibits apoptosis, and enhances metabolic activity, which are characteristic features of hyperthyroidism [39].Akt has also been found to regulate the expression and activity of key thyroid hormone receptors, further contributing to the development of

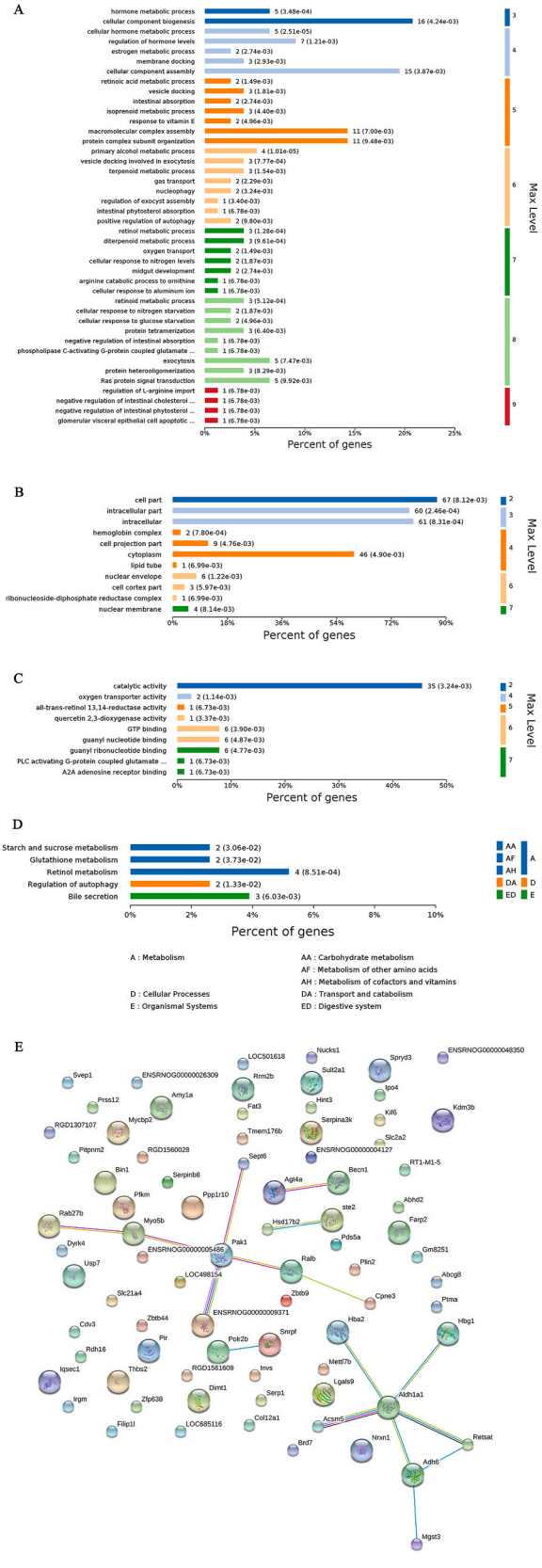

(caption on next page)

Fig. 5. GO enrichment analysis, KEGG pathway analysis, and protein–protein interaction network diagram. (A) Biological process (BP), (B) cellular component (CC), and (C) molecular function (MF) terms. (D) The node size indicates the number of connections (degree), and the node color indicates the betweenness centrality (blue: low betweenness centrality, red: high betweenness centrality). The key proteins with the highest betweenness centrality values shown in the table are marked by the red nodes in the subnetwork. (E) Protein–protein interaction network diagram of significantly differentially expressed proteins (DEPs) at the protein level.

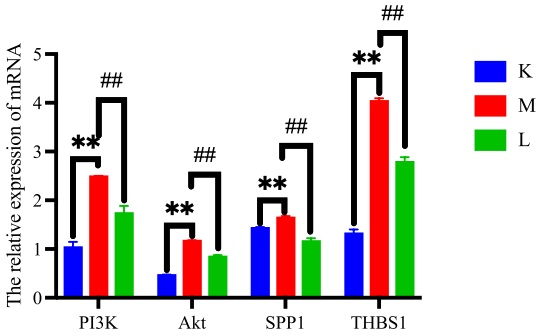

Fig. 6. Validation of the microarray data by qRT–PCR analysis (n = 3). The results are expressed as the relative quantification normalized to β-actin mRNA expression. $^{**}P < 0.01$ vs. the control group. $^{\#\#}P < 0.01$ vs. model group.

hyperthyroidism [40].

In this study, intervention with highly polar iridoids from *R. Scrophulariae* resulted in a significant decrease in the levels of Spp1, Thbs1, PI3K, and Akt. This suggests that the high-polarity iridoid glycosides from *R. Scrophulariae* may inhibit the abnormal activation of the PI3K-Akt signalling pathway by downregulating the levels of Spp1, Thbs1, PI3K, and Akt. This can reduce thyroid hormone levels in the hyperthyroid body, inhibit the proliferation and differentiation of thyroid cells, and regulate immune function to prevent and treat hyperthyroidism.

Notably, the upregulation of SPP1 and THBS1 is associated with the occurrence and development of hyperthyroidism; however, these genes are involved in this process. The pathogenesis of hyperthyroidism is highly complex and involves the regulation of multiple genes and signalling pathways. Therefore, the upregulation of a single gene or protein cannot fully explain the occurrence and development of hyperthyroidism.

The PI3K-Akt signalling pathway is a crucial cellular pathway that regulates various biological processes, including cell growth, proliferation, survival, and metabolism. Activation of this pathway can promote cell proliferation and survival while inhibiting apoptosis. Research has shown that the PI3K-Akt signalling pathway also plays a significant role in the development and progression of hyperthyroidism. Thyroid hormones can activate this pathway, leading to thyroid hyperfunction, increased cell proliferation, and metabolism [41]. Furthermore, abnormal activation of the PI3K-Akt pathway is associated with the occurrence and metastasis of tumors related to hyperthyroidism [42].

Considering the significance of the PI3K-Akt signalling pathway in hyperthyroidism, it may serve as a potential target for its treatment. Investigating the regulatory mechanisms of this pathway and its associated signalling molecules, such as SPP1 and THBS1, can enhance our understanding of the pathogenesis of hyperthyroidism and offer new insights and approaches for its treatment.

The regulation of the Spp1 gene and Thbs1 protein by the PI3K-Akt signalling pathway, along with its interactions with other signalling pathways involved in thyroid hormone homeostasis, highlights the complex network of molecular mechanisms that govern extracellular matrix remodelling and cellular responses to hormonal stimuli. Further research into these interactions may provide insights into potential therapeutic targets for diseases associated with dysregulated extracellular matrix remodelling and thyroid hormone signalling.

The PI3K-Akt signalling pathway plays a crucial role in regulating various cellular processes, including cell growth, proliferation, survival, and metabolism. This pathway is activated in response to various extracellular stimuli, such as growth factors, cytokines, and hormones, which results in the phosphorylation and activation of downstream targets, including transcription factors and other signalling molecules.

Both the Spp1 gene and Thbs1 protein are involved in extracellular matrix remodelling and are known to be regulated by the PI3K-Akt signalling pathway. The Spp1 gene encodes osteopontin, a glycoprotein involved in cell adhesion, migration, and inflammation, while Thbs1 encodes thrombospondin-1, a matricellular protein that regulates cell-matrix interactions and cell signalling [43].

The PI3K-Akt signalling pathway is involved in the regulation of the Spp1 gene and Thbs1 protein through multiple mechanisms. Akt, a crucial downstream effector of PI3K, directly phosphorylates and activates transcription factors such as NF-κB and AP-1. These transcription factors can then bind to the promoter regions of the Spp1 and Thbs1 genes, modulating their transcription [44]. Additionally, Akt can regulate the activity of other transcription factors, such as CREB and FOXO, which may also contribute to the regulation of Spp1 and Thbs1 expression [45].

In addition to the PI3K-Akt signalling pathway, other pathways involved in maintaining thyroid hormone homeostasis, such as the thyroid hormone receptor (THR) signalling pathway and the MAPK signalling pathway, may also play a role in regulating Spp1 and

Thbs1. Thyroid hormones can directly influence the expression of Spp1 and Thbs1 by binding to THR and modulating its transcriptional activity. Moreover, the MAPK signalling pathway, which can be activated by growth factors and cytokines, can cross-communicate with the PI3K-Akt pathway and regulate the expression of Spp1 and Thbs1 through shared downstream targets [46].

Spp1 and Thbs1 have attracted significant attention in the study of the PI3K/AKT signalling pathway due to their established associations with the pathway and their potential contributions to disease progression. By further investigating the expression and function of these genes, researchers can gain valuable insights into the activity of the PI3K/AKT pathway and potentially uncover novel therapeutic targets for diseases associated with pathway dysregulation.

The PI3K/AKT signalling pathway is a crucial pathway that plays a pivotal role in regulating cell growth, proliferation, survival, and metabolism. Dysregulation of this pathway has been implicated in various diseases, including cancer, diabetes, and cardiovascular diseases. Consequently, understanding the activity of the PI3K/AKT pathway and the genes associated with it is crucial for identifying potential therapeutic targets and biomarkers.

During the course of conducting a differential gene expression analysis, it is essential to identify genes that demonstrate significant differential expression between experimental conditions. In the context of studying the PI3K/AKT pathway, particular interest lies in genes that are directly regulated by or involved in the pathway. Two such genes are Spp1 (osteopontin) and Thbs1 (thrombospondin 1), which are associated with the PI3K/AKT pathway.

Spp1 is a secreted glycoprotein that participates in cell adhesion, migration, and survival. It has been reported to be upregulated in various cancers and is regulated by the PI3K/AKT pathway [34].Moreover, Spp1 has been implicated in promoting tumor growth, invasion, and metastasis, rendering it a potential target for cancer therapy. On the other hand, Thbs1 is a matricellular glycoprotein that governs cell adhesion, migration, and angiogenesis. It has been demonstrated to interact with various components of the PI3K/AKT pathway and to modulate its activity [47].Thbs1 has been associated with promoting tumor growth, angiogenesis, and metastasis in cancer and has been identified as a significant player in inflammation and fibrosis.

By conducting a PPI network analysis, valuable insights can be obtained regarding the roles of key proteins such as Pak1, Adh6, and Sept6 in relevant biological pathways, as well as their potential implications in hyperthyroidism. Gaining a comprehensive understanding of the roles of Pak1, Adh6, and Sept6 in relevant biological pathways can offer valuable insights into their potential contributions to hyperthyroidism. Further exploration of the specific interactions and functions of these proteins within the context of thyroid function and dysfunction can enhance our knowledge of the molecular mechanisms underlying hyperthyroidism and potentially pave the way for the development of targeted therapies for this condition.

Pak1 (p21-activated kinase 1) is a serine/threonine protein kinase that plays a pivotal role in diverse cellular processes, such as cell proliferation, survival, migration, and cytoskeletal dynamics. In the context of hyperthyroidism, Pak1 may be implicated in the regulation of thyroid cell growth and function, as thyroid hormone signalling pathways can activate Pak1. Furthermore, Pak1 has been associated with cancer progression, and its dysregulation may contribute to the development of thyroid cancer in individuals with hyperthyroidism [48].

Adh6 is an enzyme that catalyzes the conversion of alcohols to aldehydes or ketones predominantly in the liver. In hyperthyroidism, Adh6 may play a role in the metabolism of thyroid hormones or other endogenous compounds affected by thyroid dysfunction. Dysfunction of Adh6 activity could impact liver detoxification processes, leading to altered hormone metabolism and potential liver complications in individuals with hyperthyroidism [49].

Septins are a group of GTP-binding proteins that participate in various cellular processes, including cytokinesis, cell polarity, and vesicle trafficking. Specifically, Sept6 (Septin 6) has been implicated in the regulation of cytoskeletal organization and cell division [50]. In hyperthyroidism, Sept6 may play a role in modulating thyroid cell proliferation and differentiation, as well as potentially influencing thyroid hormone secretion and signalling pathways.

The potential anti-thyroid activity of iridoid glycosides presents new opportunities for the development of innovative therapeutic strategies for hyperthyroidism, providing the potential for more targeted and effective treatments for this prevalent endocrine disorder. Multiomics analysis demonstrated that the hyperthyroidism-induced activation of the PI3K/Akt pathway can be inhibited by highly polar iridoids from *R. Scrophulariae*. These findings indicate the involvement of the PI3K/Akt signalling pathway in the abnormal state of the rat body caused by hyperthyroidism, which is relevant to the preventative and therapeutic effects of *R. Scrophulariae* on hyperthyroidism. The findings of this study on the potential antithyroid activity of iridoid glycosides have significant implications for the development of innovative therapeutic strategies for human hyperthyroidism. Hyperthyroidism is characterized by the overactivity of the thyroid gland, resulting in excessive production of thyroid hormones. Current treatment options for hyperthyroidism include medications to inhibit thyroid hormone production or block the effects of thyroid hormones on the body. The potential anti-thyroid activity of iridoid glycosides suggests that these compounds can modulate thyroid function and may be used as a novel therapeutic approach for hyperthyroidism. By directly targeting the thyroid gland, iridoid glycosides could provide a more specific and potentially more effective treatment option for hyperthyroidism than current medications. The translation of these findings into clinical practice requires further research to determine the safety and effectiveness of iridoid glycosides in humans with hyperthyroidism. Preclinical studies evaluating the effects of iridoid glycosides on thyroid function and hormone levels, as well as clinical trials assessing their therapeutic potential in patients with hyperthyroidism, are needed.

5. Conclusions

According to transcriptomic and proteomic data, high-polarity iridoid glycosides from *R. Scrophulariae* may ameliorate hyperthyroidism by regulating the PI3K-Akt signalling pathway and modulating the Spp1 gene and Thbs1 protein. This study provides an experimental reference for the development of drugs for the prevention and treatment of hyperthyroidism. It is important to

acknowledge that this study was only a preliminary and systematic exploration at the animal, omics, and molecular levels. It should be noted that further research is required to elucidate the detailed mechanisms of factors upstream or downstream of the PI3K-Akt signalling pathway, which are associated with hyperthyroidism, as well as their connection to the prevention and treatment of hyperthyroidism.

Abbreviations

Radix	Scrophulariae R. Scrophulariae
T3	Triiodothyronine
T4	Thyroxine
TSH	thyroid-stimulating hormone
ELISA	enzyme-linked immunosorbent assay
DEGs	differentially expressed genes
RPKM	Reads Per Kilobase Million
GO	Gene Ontology
KEGG	Kyoto Encyclopedia of Genes and Genomes
DEPs	differentially expressed proteins
PPI	protein-protein interaction
qRT-PCR	Real-time quantitative reverse transcription polymerase chain reaction
DEGs	differentially expressed genes
HPLC	High Performance Liquid Chromatography
PPI	Protein-Protein Interaction
TPO	thyroid peroxidase
ACN	Acetonitrilen
Pak1	p21-activated kinase 1
Adh6	alcohol dehydrogenase 6
Sept6	septin 6
Polr2b	DNA-directed RNA polymerase II subunit RPB2
Myo5b	myosin-Vb
Hsd17b2	3alpha(17beta)-hydroxysteroid dehydrogenase (NAD+)
Hbg1	Beta-globin chain (Fragment)
Hba2	hemoglobin subunit alpha 2
Cpne3	Copine 3
Aldh1a1	aldehyde dehydrogenase 1 family member A1
Agt4a	autophagy related 4A, cysteine peptidase
Acsm5	medium-chain acyl-CoA synthetase 5
ECM	Extracellular Matrix
Spp1	secreted phosphoprotein 1
Thbs1	thrombospondin 1

Ethics approval and consent to participate

The animal study underwent a review and received approval from the Institutional Animal Ethics Committee at Heilongjiang University of Chinese Medicine.

Consent for publication

Not applicable.

Conflicts of interes

The authors declare that they do not have any competing interests.

Funding

This work was supported by grants from the National Natural Science Foundation of China (82060830), Guizhou Province Science and Technology Plan Project (QiankeheFoundation - ZK[2024] Key073) and the Major State Basic Research Development Program (973 Program) of China (2013CB531804).

Data availability statement

Data was included in supp. Material.

CRediT authorship contribution statement

Ning Zhang: Writing – review & editing, Writing – original draft, Resources, Funding acquisition, Conceptualization. **Shumin Liu:** Supervision, Conceptualization. **Xu Lu:** Writing – original draft, Data curation, Conceptualization. **Zihui Li:** Writing – original draft, Project administration, Methodology, Investigation, Data curation, Conceptualization. **Ling Li:** Writing – review & editing, Writing – original draft, Methodology, Investigation, Conceptualization. **Tao Ye:** Writing – review & editing, Writing – original draft, Supervision, Data curation, Conceptualization.

Declaration of competing interest

The authors declare that they have no known competing financial interests or personal relationships that could have appeared to influence the work reported in this paper.

Acknowledgements

Not applicable.

References

[1] W.M. Wiersinga, K.G. Poppe, G. Effraimidis, Hyperthyroidism: aetiology, pathogenesis, diagnosis, management, complications, and prognosis, Lancet Diabetes Endocrinol. 11 (4) (2023) 282–298.
[2] S.Y. Lee, E.N. Pearce, Hyperthyroidism: a review, JAMA 330 (15) (2023) 1472–1483.
[3] P. Vaidyanathan, Update on pediatric hyperthyroidism, Adv. Pediatr. 69 (1) (2022) 219–229.
[4] K. Kobaly, S.J. Mandel, Hyperthyroidism and pregnancy, Endocrinol Metab. Clin. N. Am. 48 (3) (2019) 533–545.
[5] C.P. Commission, Pharmacopoeia of the People's republic of china(Part 1), The Medicine Science and Technology Press of China, 2020, p. 121.
[6] S. Wang, et al., Simultaneous determination of iridoid glycosides, phenylpropanoid glycosides, organic acids, nucleosides and amino acids in Scrophulariae Radix processed by different processing methods by HPLC-QTRAP-MS/MS, J. Chromatogr. Sci. 60 (3) (2022) 232–242.
[7] N. Zhang, et al., Radix Scrophulariae extracts exert effect on hyperthyroidism via MST1/hippo signaling pathway, Chin. J. Integr. Med. 29 (11) (2023) 998–1006.
[8] N. Zhang, et al., Effects of Radix Scrophulariae on hyperthyroidism assessed by metabonomics and network pharmacology, Front. Pharmacol. 12 (2021) 727735.
[9] S. Kumar, et al., Phloretin and phloridzin improve insulin sensitivity and enhance glucose uptake by subverting PPARγ/Cdk5 interaction in differentiated adipocytes, Exp. Cell Res. 383 (1) (2019) 111480.
[10] J. Sharma, et al., Identification of naturally originated molecules as γ-aminobutyric acid receptor antagonist, J. Biomol. Struct. Dyn. 39 (3) (2021) 911–922.
[11] R. Singh, et al., Identification of selective cyclin-dependent kinase 2 inhibitor from the library of pyrrolone-fused benzosuberene compounds: an in silico exploration, J. Biomol. Struct. Dyn. 40 (17) (2022) 7693–7701.
[12] A. Kumar, et al., Molecular dynamic simulation reveals damaging impact of RAC1 F28L mutation in the switch I region, PLoS One 8 (10) (2013) e77453.
[13] A. Kumar, et al., Evidence of colorectal cancer-associated mutation in MCAK: a computational report, Cell Biochem. Biophys. 67 (3) (2013) 837–851.
[14] A. Kumar, et al., Computational SNP analysis: current approaches and future prospects, Cell Biochem. Biophys. 68 (2) (2014) 233–239.
[15] Z. Ning, et al., Antidiabetic activity of Radix Scrophulariae and its split fraction, Pharmacology and Clinics of Chinese Materia Medica 32 (5) (2016) 55–60.
[16] A. Rao, et al., Exploring tissue architecture using spatial transcriptomics, Nature 596 (7871) (2021) 211–220.
[17] H.M. Bennett, et al., Single-cell proteomics enabled by next-generation sequencing or mass spectrometry, Nat. Methods 20 (3) (2023) 363–374.
[18] X. hang, T. cheng, D. deqiang, Effects of 3 Chinese drugs with cold property on hyperthyrosis rats induced by Euthyrox Chinese, Archives of Traditional Chinese Medicine(中华中医药学刊) 34 (9) (2016) 2122–2125.
[19] Z. Ning, et al., The effect of Radix Scrophulariae on endogenous markers in serum of hyperthyroidism model rats, LISHIZHEN MEDICINE AND MATERIA MEDICA RESEARCH 30 (5) (2019) 1079–1083.
[20] F. Lu, et al., High throughput metabolomics-proteomics investigation on metabolic phenotype changes in rats caused by Radix Scrophulariae using ultra-performance liquid chromatography with mass spectrometry, RSC Adv. 9 (31) (2019) 17791–17800.
[21] Z. Ning, et al., Study on Radix Scrophulariae for the treatment of hyperthyroidism rat model of yin deficiency based on urine metabonomics, Acta Pharm. Sin. 53 (11) (2018) 1843–1851.
[22] Z. Ning, et al., Study on the molecular mechanism of extract from Radix Scrophulariae on hyperthyroidism rat model of yin deficiency and fire excess based on transcriptome sequencing technique, CJTCMP 37 (2) (2022) 709–713.
[23] Z. Ning, et al., Impact of extracts of Xuanshen on liver matabolome in rat model of hyperthyroidism, Journal of Beijing University of Traditional Chinese Medicine 42 (1) (2019) 21–29.
[24] Z. Ning, et al., Study of proteomics on Radix Scrophulariae for the treatment of hyperthyroidism rat model of yin deficiency with effulgent fire based on iTRAQ, CJTCMP 36 (7) (2021) 4207–4211.
[25] N. Lacámara, et al., Identification of resistance to exogenous thyroxine in humans, Thyroid 30 (12) (2020) 1732–1744.
[26] M. Srivastava, et al., Simultaneous quantification of five bioactive phenylethanoid, iridoid, and flavonol glycosides in Duranta erecta L.: ultra performance liquid chromatography method validation and uncertainty measurement, J. Pharm. Biomed. Anal. 174 (2019) 711–717.
[27] W. Zhang, et al., Protective effect and mechanism of plant-based monoterpenoids in non-alcoholic fatty liver diseases, J. Agric. Food Chem. 70 (16) (2022) 4839–4859.
[28] H. Ge, et al., Catalpol alleviates myocardial ischemia reperfusion injury by activating the Nrf2/HO-1 signaling pathway, Microvasc. Res. 140 (2022) 104302.
[29] A. Ishimitsu, et al., Eucommia ulmoides (Tochu) and its extract geniposidic acid reduced blood pressure and improved renal hemodynamics, Biomed. Pharmacother. 141 (2021) 111901.
[30] H. Lou, et al., The potential role of osteopontin in the pathogenesis of graves' ophthalmopathy, Invest. Ophthalmol. Vis. Sci. 62 (12) (2021) 18.
[31] Y. Xie, et al., Role of Thrombospondin-1 in sepsis-induced myocardial injury, Mol. Med. Rep. 24 (6) (2021).
[32] C.F. Woeller, et al., TSHR signaling stimulates proliferation through PI3K/Akt and induction of miR-146a and miR-155 in thyroid eye disease orbital fibroblasts, Invest. Ophthalmol. Vis. Sci. 60 (13) (2019) 4336–4345.
[33] S. De Schepper, et al., Perivascular cells induce microglial phagocytic states and synaptic engulfment via SPP1 in mouse models of Alzheimer's disease, Nat. Neurosci. 26 (3) (2023) 406–415.
[34] Y. Zhang, et al., microRNA-944 inhibits breast cancer cell proliferation and promotes cell apoptosis by reducing SPP1 through inactivating the PI3K/Akt pathway, Apoptosis 28 (11–12) (2023) 1546–1563.
[35] C.W. Cheng, W.F. Fang, J.D. Lin, Associations of serum keratin 1 with thyroid function and immunity in Graves' disease, PLoS One 18 (11) (2023) e0289345.

[36] M. Omatsu, et al., THBS1-producing tumor-infiltrating monocyte-like cells contribute to immunosuppression and metastasis in colorectal cancer, Nat. Commun. 14 (1) (2023) 5534.
[37] Z. Feng, et al., Differential expression of a set of microRNA genes reveals the potential mechanism of papillary thyroid carcinoma, Ann. Endocrinol. 80 (2) (2019) 77–83.
[38] A. Jin, et al., High expression of THBS1 leads to a poor prognosis in papillary thyroid cancer and suppresses the anti-tumor immune microenvironment, Technol. Cancer Res. Treat. 21 (2022) 15330338221085360.
[39] J. Sun, et al., Plasma exosomes transfer miR-885-3p targeting the AKT/NFκB signaling pathway to improve the sensitivity of intravenous glucocorticoid therapy against graves ophthalmopathy, Front. Immunol. 13 (2022) 819680.
[40] C.D. Davidson, et al., Thyroid hormone receptor beta inhibits PI3K-Akt-mTOR signaling Axis in anaplastic thyroid cancer via genomic mechanisms, J Endocr Soc 5 (8) (2021) bvab102.
[41] M. Yang, et al., Possible molecular exploration of herbal pair Haizao-Kunbu in the treatment of Graves' disease by network pharmacology, molecular docking, and molecular dynamic analysis, Front. Endocrinol. 14 (2023) 1236549.
[42] X. Xiao, et al., Methylation-mediated silencing of ATF3 promotes thyroid cancer progression by regulating prognostic genes in the MAPK and PI3K/AKT pathways, Thyroid 33 (12) (2023) 1441–1454.
[43] L. Bello, E. Pegoraro, The "usual suspects": genes for inflammation, fibrosis, regeneration, and muscle strength modify duchenne muscular dystrophy, J. Clin. Med. 8 (5) (2019).
[44] R.A. Burgos, et al., Andrographolide, an anti-inflammatory multitarget drug: all roads lead to cellular metabolism, Molecules 26 (1) (2020).
[45] Y. Wang, et al., Traxoprodil produces antidepressant-like behaviors in chronic unpredictable mild stress mice through BDNF/ERK/CREB and AKT/FOXO/bim signaling pathway, Oxid. Med. Cell. Longev. 2023 (2023) 1131422.
[46] Z. Hu, et al., Effect of grass carp scale collagen peptide FTGML on cAMP-PI3K/Akt and MAPK signaling pathways in B16F10 melanoma cells and correlation between anti-melanin and antioxidant properties, Foods 11 (3) (2022).
[47] W. Zhang, et al., MiR-3612 targeting THBS1 suppresses nasopharyngeal carcinoma progression by PI3K/AKT signaling pathway, Hum. Exp. Toxicol. 42 (2023) 9603271221150248.
[48] Y. Fan, et al., Hypermethylation of microRNA-497-3p contributes to progression of thyroid cancer through activation of PAK1/β-catenin, Cell Biol. Toxicol. 39 (5) (2023) 1979–1994.
[49] N. Chen, et al., miR-29c-3p promotes alcohol dehydrogenase gene cluster expression by activating an ADH6 enhancer, Biochem. Pharmacol. 203 (2022) 115182.
[50] C.C. Devitt, et al., PCP and Septins govern the polarized organization of the actin cytoskeleton during convergent extension, Curr. Biol. 34 (3) (2024) 615–622. e4.